

Geometry-Aware Gradient Algorithms for Neural Architecture Search

Liam Li^{*1}, Mikhail Khodak^{*1}, Maria-Florina Balcan¹, and Ameet Talwalkar^{1,2}

¹ Carnegie Mellon University

² Determined AI

me@liamcli.com, khodak@cmu.edu, ninamf@cs.cmu.edu, talwalkar@cmu.edu

Abstract. Many recent state-of-the-art methods for neural architecture search (NAS) relax the NAS problem into a joint continuous optimization over architecture parameters and their shared-weights, enabling the application of standard gradient-based optimizers. However, this training process remains poorly understood, as evidenced by the multitude of gradient-based heuristics that have been recently proposed. Invoking the theory of mirror descent, we present a unifying framework for designing and analyzing gradient-based NAS methods that exploit the underlying problem structure to quickly find high-performance architectures. Our *geometry-aware* framework leads to simple yet novel algorithms that (1) enjoy faster convergence guarantees than existing gradient-based methods and (2) achieve state-of-the-art accuracy on the latest NAS benchmarks in computer vision. Notably, we exceed the best published results for both CIFAR and ImageNet on both the DARTS search space and NAS-Bench-201; on the latter benchmark we achieve close to oracle-optimal performance on CIFAR-10 and CIFAR-100.³ Together, our theory and experiments demonstrate a principled way to co-design optimizers and continuous parameterizations of discrete NAS search spaces.

1 Introduction

Neural architecture search has become an important tool for automating machine learning (ML) [43, 9] but can require hundreds of thousands of GPU-hours to train and contribute hundreds of thousands of kilograms to CO₂ emissions [46]. Recently, approaches based on *weight-sharing* have achieved state-of-the-art performance on canonical image classification and language modeling problems while drastically reducing the computational cost of NAS to just that of training a single *shared-weights network* [40, 29, 32]. Crucially, methods such as DARTS [32], GDAS [17], and many others [40, 57, 51, 39, 48, 31, 27, 9, 37, 3, 49] combine weight-sharing with a continuous relaxation of the discrete search space to allow cheap gradient updates to architecture hyperparameters, enabling the use of popular optimizers

³ Code available at https://github.com/liamcli/gaea_release.

* Denotes equal contribution.

such as stochastic gradient descent (SGD) or Adam [23]. However, despite some empirical success, weight-sharing remains poorly understood and subsequent improvements to the search process continue to be largely heuristic [39, 37, 10, 30, 28, 49, 54]. Furthermore, on recent computer vision benchmarks weight-sharing methods can still be outperformed by traditional hyperparameter tuning algorithms given a similar time-budget [18]. Thus, motivated by the challenge of developing simple, efficient, and sustainable NAS methods that achieve *state-of-the-art* performance in computer vision and beyond, we make progress on the following question: *how can we design and analyze fast and accurate methods for NAS with weight-sharing?*

We start from the observation that methods that use weight-sharing subsume architecture hyperparameters as another set of learned parameters of the shared-weights network, in effect extending the class of functions being learned. This insight reduces our motivating question to the following: *how can we design and analyze fast and accurate methods for empirical risk minimization (ERM) over this extended class?* While this is a well-studied problem in ML and procedures such as SGD have been remarkably effective for unconstrained neural network optimization [47], it is far from clear that this will naturally extend to optimizing architecture parameters, which can lie in constrained, non-Euclidean domains.

In this paper we argue for and develop a more principled, *geometry-aware* framework for designing and analyzing both continuous relaxations and optimizers for NAS with weight-sharing. Drawing upon the mirror descent meta-algorithm [38, 6], we give polynomial-time convergence guarantees when optimizing the weight-sharing objective for a broad class of gradient-based methods that connect to the underlying problem structure. Notably, this allows us to reason about (1) the speed of both new and existing NAS methods, and (2) how to construct continuous relaxations of discrete search spaces. We use this framework to design state-of-the-art NAS methods, as detailed below in our contributions:

1. We formulate the optimization of NAS with weight-sharing as ERM over a structured function class in which architectural decisions are treated as learned parameters rather than hyperparameters. We prove polynomial-time stationary-point convergence guarantees for block-stochastic mirror descent over a continuous relaxation of this objective and show that gradient-based methods such as ENAS [40] and DARTS [32] can be viewed as variants of this meta-algorithm. To the best of our knowledge these are the first finite-time convergence guarantees for any gradient-based NAS method.
2. Crucially, the convergence rates we prove depend on the underlying architecture parameterization. We thus propose to improve upon existing NAS algorithms by (1) using different continuous relaxations of the discrete search space and (2) applying mirror descent procedures adapted to these new geometries. Our instantiation of this approach—which we call the **Geometry-Aware Exponentiated Algorithm (GAEA)**—is a simple modification applicable to many methods including first-order DARTS, PC-DARTS [49], and GDAS [17]. It constrains architecture parameters to the simplex and

- updates them using exponentiated gradient, a variant of mirror descent that converges quickly over this domain and enjoys favorable sparsity properties.
3. We demonstrate that GAEA improves upon state-of-the-art methods on three of the latest NAS benchmarks for computer vision.⁴ Specifically, we beat the current best results on NAS-Bench-201 [18] by 0.18% on CIFAR-10, 1.59% on CIFAR-100, and 0.82% on ImageNet-16-120; we also outperform the state-of-the-art on the DARTS search space [32], for both CIFAR-10 and ImageNet, and match it on NAS-Bench-1Shot1 [55].

1.1 Related Work

Most analyses of optimization problems associated with NAS show monotonic improvement [3], asymptotic guarantees [52], or bounds on auxiliary quantities, e.g. regret, that are not well-connected to the objective [39, 37, 10]. In contrast, we prove polynomial-time stationary-point convergence on the single-level (ERM) objective for NAS with weight-sharing, which is effective in practice. Furthermore, due to the generality of mirror descent, our results can be applied to previously un-analyzed methods such as first-order DARTS [32] and ENAS [40]. Finally, we note that a variant of GAEA that modifies first-order DARTS is related to XNAS [37], whose update also involves an exponentiated gradient step; however, GAEA is simpler and easier to implement.⁵ Furthermore, the regret guarantees for XNAS do not relate to any meaningful performance measure for NAS such as speed or accuracy, whereas we guarantee convergence on the ERM objective.

Our results draw upon the extensive literature on first-order optimization [5] in particular on the mirror descent meta-algorithm [38, 6]. Such methods have been successfully used in a wide array of applications in machine learning [1, 35, 14], computer vision [26, 33, 2], and theoretical computer science [4, 41, 8]. We extend recent nonconvex convergence guarantees for stochastic mirror descent [56] to handle alternating descent schemes; while there exist related results in this setting [13] the associated guarantees do not hold for the algorithms we propose.

2 The Weight-Sharing Optimization Problem

In standard supervised ML we are given a dataset T of labeled pairs (x, y) drawn from a distribution \mathcal{D} over input space X and output space Y . The goal is to use this data to search some parameterized function class H for a function $h_{\mathbf{w}} : X \mapsto Y$ parameterized by $\mathbf{w} \in \mathbb{R}^d$ that has low expected test loss $\ell(h_{\mathbf{w}}(x), y)$ when using x to predict the associated y on unseen samples drawn from the same

⁴ All associated code and environments will be released for reproducibility.

⁵ Code provided for XNAS (<https://github.com/NivNayman/XNAS>) does not implement the search algorithm and, as with previous efforts [28, OpenReview Forum], we were unable to reproduce the reported search results after correspondence with the authors. The best architecture reported by XNAS achieves an average test error of 2.70% under the DARTS evaluation protocol, while GAEA achieves 2.50%. We provide further discussion and experimental comparison with XNAS in the appendix.

distribution, as measured by some loss function $\ell : Y \times Y \mapsto [0, \infty)$. A common way to do this is (regularized) ERM, which outputs $\mathbf{w} \in \mathbb{R}^d$ such that $h_{\mathbf{w}} \in H$ has the smallest average (regularized) loss over the training sample T .

2.1 Single-Level Neural Architecture Search

NAS is often viewed as hyperparameter optimization on top of ERM [29], with each architecture $a \in \mathcal{A}$ corresponding to a function class H_a to be selected via validation data. However, unlike hyperparameters such as regularization and step-size, these architectural hyperparameters directly affect the mapping from X to Y , so one can forgo holding out validation data and find the best function in $H_{\mathcal{A}} = \bigcup_{a \in \mathcal{A}} H_a = \{h_{\mathbf{w},a} : X \mapsto Y, \mathbf{w} \in \mathbb{R}^d, a \in \mathcal{A}\}$. Formally, for some regularization parameter $\lambda \geq 0$, we solve

$$\min_{\mathbf{w} \in \mathbb{R}^d, a \in \mathcal{A}} \lambda \|\mathbf{w}\|_2^2 + \frac{1}{|T|} \sum_{(x,y) \in T} \ell(h_{\mathbf{w},a}(x), y) \quad (1)$$

Under this formulation, the use of weight-sharing is perhaps not surprising: both the network parameters \mathbf{w} and architecture decisions a are part of the same optimization domain. This is made even more clear in the common approach where the discrete decision space is relaxed into a continuous one and the optimization becomes one over some subset Θ of a finite-dimensional real vector space:

$$\min_{\mathbf{w} \in \mathbb{R}^d, \theta \in \Theta} \lambda \|\mathbf{w}\|_2^2 + \frac{1}{|T|} \sum_{(x,y) \in T} \ell(h_{\mathbf{w},\theta}(x), y) \quad (2)$$

Here $h_{\mathbf{w},\theta} : X \mapsto Y$ is determined by some superposition of architectures, such as the θ -weighted mixture on each edge used by DARTS [32] or the randomized function with θ -parameterized distribution employed by GDAS [17]; this is detailed in Section 2.2. Note that in order for the relaxation (2) to be a useful surrogate for (1), we need a (possibly randomized) mapping from a feasible point $\theta \in \Theta$ to $a \in \mathcal{A}$; the associated error or variance of this mapping can be catastrophic, as witnessed by the performance of DARTS on NAS-Bench-201 [18].

This analysis reduces our motivating questions from the introduction to the following: *how do we design a relaxation Θ of architecture space \mathcal{A} that admits an optimizer that is simultaneously fast at solving (2) and leads to parameters $\theta \in \Theta$ that can be mapped to architectures $a \in \mathcal{A}$ with low test error?* In the sequel, we provide an answer using the mirror descent framework.

Before proceeding, we note that many weight-sharing approaches [40, 32, 17] attempt to solve a *bilevel* problem rather than ERM by using a validation set V :

$$\begin{aligned} & \min_{\mathbf{w} \in \mathbb{R}^d, \theta \in \Theta} \frac{1}{|V|} \sum_{(x,y) \in V} \ell(h_{\mathbf{w},\theta}(x), y) \\ \text{s.t. } & \mathbf{w} \in \arg \min_{\mathbf{u} \in \mathbb{R}^d} \lambda \|\mathbf{u}\|_2^2 + \frac{1}{|T|} \sum_{(x,y) \in T} \ell(h_{\mathbf{u},\theta}(x), y) \end{aligned} \quad (3)$$

Here our theory does not hold,⁶ but we believe that our guarantees for block-stochastic methods—the heuristic of choice for modern bilevel problems [19, 32]—are still useful for algorithm design. Furthermore, past work has sometimes used the single-level approach [48, 28] and we find it very effective on some benchmarks.

2.2 Neural Architecture Search with Weight-Sharing

We next review the NAS setup motivating our work. Weight-sharing methods almost exclusively use micro cell-based search spaces for their tractability and additional structure [40, 32]. These search spaces can be represented as directed acyclic graphs (DAGs) with a set of ordered nodes N and edges E . Each node $x^{(i)} \in N$ is a feature representation and each edge $(i, j) \in E$ is associated with an operation on the feature of node j passed to node i and aggregated with other inputs to form $x^{(j)}$, with the restriction that a given node j can only receive edges from prior nodes as input. Hence, the feature at node i is $x^{(i)} = \sum_{j < i} o^{(i,j)}(x^{(j)})$. Search spaces are specified by the number of nodes, the number of edges per node, and the set of operations O that can be applied at each edge. Thus for NAS, $\mathcal{A} \subset \{0, 1\}^{|E| \times |O|}$ is the set of all valid architectures for encoded by edge and operation decisions. Treating both the *shared weights* $\mathbf{w} \in \mathbb{R}^d$ and architecture decisions $a \in \mathcal{A}$ as parameters, weight-sharing methods train a single network subsuming all possible functions within the search space.

Gradient-based weight-sharing methods apply continuous relaxations to the architecture space \mathcal{A} in order to compute gradients in a continuous space Θ . Methods like DARTS [32] and its variants [11, 27, 22, 30, 39, 37] relax the search space by considering a *mixture* of operations per edge. For example, we will consider a relaxation where the architecture space $\mathcal{A} = \{0, 1\}^{|E| \times |O|}$ is relaxed into $\Theta = [0, 1]^{|E| \times |O|}$ with the constraint that $\sum_{o \in O} \theta_{i,j,o} = 1$, i.e. the operation weights on each edge sum to 1. The feature at node i is then $x^{(i)} = \sum_{j < i} \sum_{o \in O} \theta_{i,j,o} o(x^{(j)})$. To get a valid architecture $a \in \mathcal{A}$ from a mixture θ , rounding and pruning are typically employed after the search phase.

An alternative, *stochastic* approach, such as that used by GDAS [17], instead uses Θ -parameterized distributions p_θ over \mathcal{A} to sample architectures [40, 48, 3, 9]; unbiased gradients w.r.t. $\theta \in \Theta$ can be computed using Monte Carlo sampling. The goal of all these relaxations is to use simple gradient-based approaches to approximately optimize (1) over $a \in \mathcal{A}$ by optimizing (2) over $\theta \in \Theta$ instead. However, both the relaxation and the optimizer critically affect the convergence speed and solution quality. We next present a principled approach for understanding both mixture and stochastic methods.

3 Geometry-Aware Gradient Algorithms

Recall that we want a fast algorithm that minimizes the regularized empirical risk $f(\mathbf{w}, \theta) = \lambda \|\mathbf{w}\|_2^2 + \frac{1}{|T|} \sum_{(x,y) \in T} \ell(h_{\mathbf{w},\theta}(x), y)$ over shared-weights $\mathbf{w} \in \mathbb{R}^d$

⁶ Known guarantees for gradient-based bilevel optimization are asymptotic and rely on strong assumptions such as uniqueness of the minimum of the inner optimization [19].

and architecture parameters $\theta \in \Theta$. We assume that we can take noisy derivatives of f separately w.r.t. either \mathbf{w} and θ at any point $(\mathbf{w}, \theta) \in \mathbb{R}^d \times \Theta$, i.e. stochastic gradients $\tilde{\nabla}_{\mathbf{w}} f(\mathbf{w}, \theta)$ or $\tilde{\nabla}_{\theta} f(\mathbf{w}, \theta)$ satisfying $\mathbb{E} \tilde{\nabla}_{\mathbf{w}} f(\mathbf{w}, \theta) = \nabla_{\mathbf{w}} f(\mathbf{w}, \theta)$ or $\mathbb{E} \tilde{\nabla}_{\theta} f(\mathbf{w}, \theta) = \nabla_{\theta} f(\mathbf{w}, \theta)$, respectively. In practice this is done by minibatch sampling of datapoints from T . Our goal will be to make the function f small while taking as few stochastic gradients as possible, although in the nonconvex case we must settle for finding a point $(\mathbf{w}, \theta) \in \mathbb{R}^d \times \Theta$ with a small gradient.

3.1 Background on Mirror Descent

While there are many ways of motivating, formulating, and describing mirror descent [38, 6, 45], for simplicity we consider the proximal formulation. The starting point here is the observation that, in the unconstrained case, performing an SGD update at a point $\theta \in \Theta = \mathbb{R}^k$ given a stochastic gradient estimate $\tilde{\nabla} f(\theta)$ with learning rate $\eta > 0$ is equivalent to solving the following proximally regularized optimization problem:

$$\theta - \eta \tilde{\nabla} f(\theta) = \arg \min_{\mathbf{u} \in \mathbb{R}^k} \eta \tilde{\nabla} f(\theta) \cdot \mathbf{u} + \frac{1}{2} \|\mathbf{u} - \theta\|_2^2 \quad (4)$$

Here the first term aligns the output with the gradient while the second (proximal) term regularizes for closeness to the previous point as measured by the Euclidean distance. While the SGD update has been found to work well for unconstrained high-dimensional optimization, e.g. deep net training, this choice of proximal regularization may be sub-optimal over a constrained space with sparse solutions.

The canonical setting where replacing gradient descent by a geometry-aware algorithm gives a concrete benefit is when we are optimizing a function over the unit simplex, i.e. when $\Theta = \{\theta \in [0, 1]^k : \|\theta\|_1 = 1\}$. Here, if we replace the ℓ_2 -regularizer in Equation 4 by the relative entropy $\mathbf{u} \cdot (\log \mathbf{u} - \log \theta)$, i.e. the Kullback-Liebler (KL) divergence between \mathbf{u} and θ , then we obtain the exponentiated gradient (EG) update:

$$\theta \odot \exp(-\eta \tilde{\nabla} f(\theta)) \propto \arg \min_{\mathbf{u} \in \Theta} \eta \tilde{\nabla} f(\theta) \cdot \mathbf{u} + \mathbf{u} \cdot (\log \mathbf{u} - \log \theta) \quad (5)$$

Note that the full EG update is obtained by normalizing the left-hand side using the ℓ_1 -norm. A classical result in convex optimization states that EG over the k -dimensional simplex requires only $\mathcal{O}(\log k/\varepsilon^2)$ iterations to achieve a function value ε -away from optimal [6, Theorem 5.1], compared to the $\mathcal{O}(k/\varepsilon^2)$ guarantee of gradient descent. This nearly dimension-independent iteration complexity is achieved by choosing a regularizer—the KL divergence—well-suited to the underlying geometry—the simplex.

In full generality, mirror descent algorithms are specified by a distance-generating function (DGF) ϕ on Θ , which should be strongly-convex w.r.t. some suitable norm $\|\cdot\|$ in order to provide geometry-aware regularization. The DGF ϕ induces a *Bregman divergence* $D_{\phi}(\mathbf{u}|\mathbf{v}) = \phi(\mathbf{u}) - \phi(\mathbf{v}) - \nabla \phi(\mathbf{v}) \cdot (\mathbf{u} - \mathbf{v})$ [7], a notion of distance on Θ that acts as a regularizer in the mirror descent update:

$$\arg \min_{\mathbf{u} \in \Theta} \eta \tilde{\nabla} f(\theta) \cdot \mathbf{u} + D_{\phi}(\mathbf{u}|\theta) \quad (6)$$

Algorithm 1: Block-stochastic mirror descent optimization of a function $f : \mathbb{R}^d \times \Theta \mapsto \mathbb{R}$, where Θ has an associated DGF ϕ .

```

Input: initialization  $(\mathbf{w}^{(1)}, \theta^{(1)}) \in \mathbb{R}^d \times \Theta$ , no. of steps  $T \geq 1$ , step-size  $\eta > 0$ 
for iteration  $t = 1, \dots, T$  do
    sample  $b_t \sim \text{Unif}\{\mathbf{w}, \theta\}$  // randomly select update block
    if block  $b_t = \mathbf{w}$  then
         $\mathbf{w}^{(t+1)} \leftarrow \mathbf{w}^{(t)} - \eta \tilde{\nabla}_{\mathbf{w}} f(\mathbf{w}^{(t)}, \theta^{(t)})$  // SGD update to shared weights
         $\theta^{(t+1)} \leftarrow \theta^{(t)}$  // no update to architecture parameters
    else
         $\mathbf{w}^{(t+1)} \leftarrow \mathbf{w}^{(t)}$  // no update to shared weights
         $\theta^{(t+1)} \leftarrow \arg \min_{\mathbf{u} \in \Theta} \eta \tilde{\nabla}_{\theta} f(\mathbf{w}^{(t)}, \theta^{(t)}) \cdot \mathbf{u} + D_{\phi}(\mathbf{u} || \theta^{(t)})$ 
        // mirror descent update to architecture parameters
    Output:  $(\mathbf{w}^{(r)}, \theta^{(r)})$  for  $r \sim \text{Unif}\{1, \dots, T\}$  // return random iterate

```

For example, to recover the SGD update (4) we can set $\phi(\mathbf{u}) = \frac{1}{2} \|\mathbf{u}\|_2^2$, which is strongly-convex w.r.t. the Euclidean norm, while the EG update (5) can be recovered by setting $\phi(\mathbf{u}) = \mathbf{u} \cdot \log \mathbf{u}$, which is strongly-convex w.r.t. the ℓ_1 -norm. As we will see, the latter regularizer is useful for obtaining sparse solutions after only a few iterations.

3.2 Block-Stochastic Mirror Descent

In the previous section we saw how mirror descent can yield fast convergence over certain geometries such as the simplex. However, in NAS with weight-sharing we are often interested in optimizing over a hybrid geometry, e.g. one containing both the shared weights in an unconstrained Euclidean space and the architecture parameters in a potentially non-Euclidean domain. Thus we focus on the optimization of a non-convex function over two blocks: shared weights $\mathbf{w} \in \mathbb{R}^d$ and architecture parameters $\theta \in \Theta$, where Θ is associated with a DGF ϕ that is strongly-convex w.r.t. some norm $\|\cdot\|$. In NAS a common approach is to perform alternating gradient steps on each domain; for example, both ENAS [40] and first-order DARTS [32] alternate between SGD updates to the shared weights and Adam [23] updates to the architecture parameters. This type of approach is encapsulated in the block-stochastic algorithm described in Algorithm 1, which at each iteration chooses one block at random to update using mirror descent (recall that SGD is also a variant of mirror descent) and after T such steps returns a random iterate. Note that Algorithm 1 subsumes both ENAS and first-order DARTS if SGD is used over the architecture parameters instead of Adam, with the following mild caveats: in practice blocks are picked cyclically rather than randomly and the algorithm returns the last iterate rather than a random one.

In Section 4 we prove that, under some assumptions on the objective f , the output $(\mathbf{w}^{(r)}, \theta^{(r)})$ of Algorithm 1 is an ε -stationary-point of f if we run at least $T = \mathcal{O}(G_{\mathbf{w}}^2 + G_{\theta}^2) / \varepsilon^2$ iterations; here $\varepsilon > 0$ measures the expected non-stationarity,

$G_{\mathbf{w}}^2$ upper-bounds the expected squared ℓ_2 -norm of the stochastic gradient $\tilde{\nabla}_{\mathbf{w}}$ w.r.t. the shared weights, and G_{θ}^2 upper-bounds the expected squared magnitude of the stochastic gradient $\tilde{\nabla}_{\theta}$ w.r.t. the architecture parameters, as measured by the *dual norm* $\|\cdot\|_*$ of $\|\cdot\|$.

This last term G_{θ} is key to understanding the usefulness of mirror descent, as it is the only term that is affected by our choice of DGF ϕ , which is strongly-convex w.r.t. $\|\cdot\|$ (recall from Section 3.1 that a variant of mirror descent is defined by its DGF). In the case of SGD, $\phi(\mathbf{u}) = \frac{1}{2}\|\mathbf{u}\|_2^2$ is strongly-convex w.r.t. the ℓ_2 -norm, which is its own dual norm; this is why $G_{\mathbf{w}}^2$ is defined via the ℓ_2 -norm of the shared weights gradient. However, in the case of exponentiated gradient $\phi(\mathbf{u}) = \mathbf{u} \cdot \log \mathbf{u}$ is strongly-convex w.r.t. the ℓ_1 -norm, whose dual norm is the ℓ_{∞} -norm. Since the ℓ_2 -norm of a k -dimensional vector can be a factor \sqrt{k} larger than its ℓ_{∞} -norm, and is never smaller, picking a DGF that is strongly-convex w.r.t. the ℓ_1 -norm can lead to much better bound on G_{θ} and thus in-turn on the number of iterations needed to reach a stationary point.

3.3 A Single-Level Analysis of ENAS and DARTS

Before using this analysis for new NAS algorithms, we first apply it to existing methods, specifically ENAS [40] and DARTS [32]. For simplicity, we assume objectives induced by architectures in the relaxed search space are γ -smooth, which excludes components such as ReLU. However, such cases can be smoothed via Gaussian convolution, i.e. adding noise to every gradient; thus given the noisiness of SGD training we believe the following analysis is still informative [24].

ENAS continuously relaxes \mathcal{A} via a neural controller that samples architectures $a \in \mathcal{A}$, so $\Theta = \mathbb{R}^{\mathcal{O}(h^2)}$, where h is the number of hidden units. The controller is trained with Monte Carlo gradients. On the other hand, first-order DARTS uses a mixture relaxation similar to the one in Section 2.2 but using a softmax instead of constraining parameters to the simplex. Thus $\Theta = \mathbb{R}^{|E| \times |O|}$ for E the set of learnable edges and O the set of possible operations. If we assume that both algorithms use SGD for the architecture parameters then to compare them we are interested in their respective values of G_{θ} , which we will refer to as G_{ENAS} and G_{DARTS} . Before proceeding, we note again that our theory holds only for the single-level objective and when using SGD as the architecture optimizer, whereas both algorithms specify the bilevel objective and Adam [23], respectively.

At a very high level, the Monte Carlo gradients used by ENAS are known to be high-variance, so G_{ENAS} may be much larger than G_{DARTS} , yielding faster convergence for DARTS, which is reflected in practice [32]. We can also do a simple low-level analysis under the assumption that all architecture gradients are bounded entry-wise, i.e. in ℓ_{∞} -norm, by some constant; then since the squared ℓ_2 -norm is bounded by the product of the dimension and the squared ℓ_{∞} -norm we have $G_{\text{ENAS}}^2 = \mathcal{O}(h^2)$ while $G_{\text{DARTS}}^2 = \mathcal{O}(|E||O|)$. Since ENAS uses a hidden state size of $h = 100$ and the DARTS search space has $|E| = 14$ edges and $|O| = 7$ operations, this also points to DARTS needing fewer iterations to converge.

3.4 GAEA: A Geometry-Aware Exponentiated Algorithm

Equipped with a general understanding block-stochastic optimizers for NAS, we now turn to designing new methods. Our goal is to pick architecture parameterizations and algorithms that (a) have fast convergence in appropriate geometries and (b) encourage favorable properties in the learned parameters. To do so, we return to the exponentiated gradient (EG) update discussed in Section 3.1 and propose **GAEA**, a **Geometry-Aware Exponentiated Algorithm** in which operation weights on each edge are constrained to the simplex and trained using EG, i.e. mirror descent with the entropic DGF $\phi(\mathbf{u}) = \mathbf{u} \cdot \log \mathbf{u}$; as in DARTS [32], the shared weights \mathbf{w} are trained using SGD.

GAEA can be used as a simple, principled modification to the many NAS methods that treat architecture parameters $\theta \in \Theta = \mathbb{R}^{|E| \times |O|}$ as real-valued “logits” to be passed through a softmax to obtain mixture weights or probabilities lying in simplices over the set of operations O . Such methods include DARTS, PC-DARTS [49], and GDAS [17]. To apply GAEA, we first re-parameterize Θ to be the product set of $|E|$ simplices, each associated to an edge $(i, j) \in E$; thus $\theta_{i,j,o}$ corresponds directly to the weight or probability of operation $o \in O$ for edge (i, j) , not an associated logit value. Then, given a stochastic gradient $\tilde{\nabla}_{\theta} f(\mathbf{w}^{(t)}, \theta^{(t)})$ and step-size $\eta > 0$, we replace the architecture update by EG:

$$\begin{aligned} \tilde{\theta}^{(t+1)} &\leftarrow \theta^{(t)} \odot \exp\left(-\eta \tilde{\nabla}_{\theta} f(\mathbf{w}^{(t)}, \theta^{(t)})\right) && \text{(multiplicative update)} \\ \theta_{i,j,o}^{(t+1)} &\leftarrow \frac{\tilde{\theta}_{i,j,o}^{(t+1)}}{\sum_{o' \in O} \tilde{\theta}_{i,j,o'}^{(t+1)}} \quad \forall o \in O, \forall (i, j) \in E && \text{(simplex projection)} \end{aligned} \quad (7)$$

These two simple modifications, *re-parameterization* and *exponentiation*, suffice to obtain state-of-the-art results on several NAS benchmarks, as shown in Section 5.

To analyze GAEA, note that the above update (7) is equivalent to mirror descent (6) with $\phi(\theta) = \sum_{(i,j) \in E} \sum_{o \in O} \theta_{i,j,o} \log \theta_{i,j,o}$, which is strongly-convex w.r.t. the norm $\|\cdot\|_1 / \sqrt{|E|}$ over the product of $|E|$ simplices of size $|O|$. The dual norm is $\sqrt{|E|} \|\cdot\|_{\infty}$, so if as before $G_{\mathbf{w}}$ bounds the gradient w.r.t. the shared weights \mathbf{w} and we have an entry-wise bound on the architecture gradient then GAEA needs $\mathcal{O}(G_{\mathbf{w}}^2 + |E|) / \varepsilon^2$ iterations to reach ε -stationary-point. This can be up to a factor $|O|$ improvement over just using SGD, e.g. the DARTS bound in Section 3.3. In addition to fast convergence, GAEA encourages sparsity in the architecture weights by using a multiplicative update over simplices and not an additive update over $\mathbb{R}^{|E| \times |O|}$, reducing the effect of post-hoc pruning or sampling when obtaining a valid architecture $a \in \mathcal{A}$ from θ . Obtaining sparse final architecture parameters is critical for good performance, both for the mixture relaxation, where it alleviates the effect of overfitting, and for the stochastic relaxation, where it reduces noise when sampling architectures.

4 Convergence of Block-Stochastic Mirror Descent

Here we give a self-contained formalization of the Algorithm 1 guarantees governing the analysis in Section 3. We start with the following regularity assumptions:

Assumption 1 *Suppose ϕ is strongly-convex w.r.t. some norm $\|\cdot\|$ on a convex set Θ and the objective function $f : \mathbb{R}^d \times \Theta \mapsto [0, \infty)$ satisfies the following:*

1. $f(\mathbf{w}, \theta) + \frac{\gamma}{2} \|\mathbf{w}\|_2^2 + \gamma\phi(\theta)$ is convex on $\mathbb{R}^d \times \Theta$ for some $\gamma > 0$.
2. $\mathbb{E}\|\tilde{\nabla}_{\mathbf{w}}f(\mathbf{w}, \theta)\|_2^2 \leq G_{\mathbf{w}}^2$ and $\mathbb{E}\|\tilde{\nabla}_{\theta}f(\mathbf{w}, \theta)\|_*^2 \leq G_{\theta}^2$ for some $G_{\mathbf{w}}, G_{\theta} \geq 0$.

The first condition, γ -relatively-weak-convexity [56], allows all γ -smooth nonconvex functions and certain non-smooth ones. The second bounds the expected stochastic gradient on each block. We also require a convergence measure; in the unconstrained case we could just use the gradient norm, but for constrained Θ the gradient may never be zero. Thus we use the *Bregman stationarity* [56, Equation 2.11], which uses the proximal operator prox_{λ} to encode non-stationarity:

$$\Delta_{\lambda}(\mathbf{w}, \theta) = \frac{D_{\ell_2, \phi}(\mathbf{w}, \theta \| \text{prox}_{\lambda}(\mathbf{w}, \theta)) + D_{\ell_2, \phi}(\text{prox}_{\lambda}(\mathbf{w}, \theta) \| \mathbf{w}, \theta)}{\lambda^2} \quad (8)$$

Here $\lambda = \frac{1}{2\gamma}$, $D_{\ell_2, \phi}$ is the Bregman divergence of the DGF $\frac{1}{2}\|\mathbf{w}\|_2^2 + \phi(\theta)$, and $\text{prox}_{\lambda}(\mathbf{w}, \theta) = \arg \min_{\mathbf{u} \in \mathbb{R}^d \times \Theta} \lambda f(\mathbf{u}) + D_{\ell_2, \phi}(\mathbf{u} \| \mathbf{w}, \theta)$; note that the dependence of the measure on γ is standard [13, 56]. Roughly speaking, if the Bregman stationarity is $\mathcal{O}(\varepsilon)$ then (\mathbf{w}, θ) is $\mathcal{O}(\varepsilon)$ -close to an $\mathcal{O}(\varepsilon)$ -approximate stationary-point [15]; in the smooth case over Euclidean geometries, i.e. SGD, if $\Delta_{\frac{1}{2\gamma}} \leq \varepsilon$ then we have an $\mathcal{O}(\varepsilon)$ -bound on the squared gradient norm, recovering the standard definition of ε -stationarity.

Theorem 1 *Let $F = f(\mathbf{w}^{(1)}, \theta^{(1)})$ be the value of f at initialization. Under Assumption 1, if we run Algorithm 1 for $T = \frac{16\gamma F}{\varepsilon^2}(G_{\mathbf{w}}^2 + G_{\theta}^2)$ iterations with step-size $\eta = \sqrt{\frac{4F}{\gamma(G_{\mathbf{w}}^2 + G_{\theta}^2)T}}$ then $\mathbb{E}\Delta_{\frac{1}{2\gamma}}(\mathbf{w}^{(r)}, \theta^{(r)}) \leq \varepsilon$. Here the expectation is over the randomness of the algorithm and over that of the stochastic gradients.*

The proof in the appendix follows from a single-block analysis of mirror descent [56, Theorem 3.1] and in fact holds for the general case of any finite number of blocks associated to any set of strongly-convex DGFs. Although there are prior results for the multi-block case [13], they do not hold for nonsmooth Bregman divergences such as the KL divergence, which we need for exponentiated gradient.

5 Empirical Results using GAEA

We evaluate GAEA, our geometry-aware NAS method, on three different computer vision benchmarks: the CNN search space from DARTS [32], NAS-Bench-1Shot1 [55], and NAS-Bench-201 [18]. Since GAEA can modify a variety of NAS methods, e.g. DARTS, PC-DARTS [49], and GDAS [17], on each benchmark we start by evaluating the GAEA variant of the current state-of-the-art method on

that benchmark. We conclude with an empirical study of the convergence of the architecture parameters of GAEA compared to that of the methods it modifies.

The three benchmarks we use comprise a diverse and complementary set of leading NAS search spaces for computer vision problems. The DARTS search space is large and heavily-studied [37, 11, 48, 39, 30, 49], while NAS-Bench-1Shot1 and NAS-Bench-201 are smaller benchmarks that allow for oracle evaluation of weight-sharing algorithms. NAS-Bench-1Shot1 differs from the other two by applying operations per node instead of per edge, while NAS-Bench-201 differs by not requiring edge-pruning. We show that despite this diversity, GAEA is able to improve upon the state-of-the-art across all three search spaces.

Due to space limitations, we defer details of the experimental setup and hyperparameter settings used for GAEA to the appendix. We note that we use the same learning rate for GAEA variants of DARTS/PC-DARTS and do not require additional weight-decay for architecture parameters. Furthermore, in the interest of reproducibility, we will be releasing all code, hyperparameters, and random seeds for our experiments.

5.1 GAEA on the DARTS Search Space

We evaluate GAEA on the task of designing CNN cells for both CIFAR-10 [25] and ImageNet [44] by modifying PC-DARTS [49], the current state-of-the-art method, to use the simplex parameterization along with exponentiated gradient (7) for the architecture parameters. We consider the same search space as DARTS [32], and follow the same three stage process used by both DARTS and random search with weight-sharing [29] for search and architecture evaluation.

GAEA PC-DARTS on CIFAR-10 As shown in Table 1, GAEA PC-DARTS finds an architecture that achieves lower error than comparably sized AmoebaNet-B and NASNet-A architectures, which required thousands of GPU days in search cost. We also demonstrate that geometry-aware co-design of the architecture parameterization and optimization scheme improves upon the original PC-DARTS, which uses Adam [23] to optimize a softmax parameterization. GAEA PC-DARTS also outperforms all non-manual methods except ProxylessNAS [9], which takes 40 times as much time, uses 1.5 times as many parameters, and is run on a different search space. Thus on the DARTS search space itself our results improve upon the state-of-the-art.

To meet a higher bar for reproducibility, we report ‘broad reproducibility’ results [29] by repeating the entire 3 stage pipeline for GAEA PC-DARTS on additional sets of seeds in the appendix. Our results show that while GAEA PC-DARTS is consistently able to find good architectures when selecting the best architecture across four independent weight-sharing trials, multiple trials are required due to sensitivity to the initialization of the weight-sharing network, as is the case for many weight-sharing approaches [32, 49].

Architecture	Source	Test Error		Params (M)	Search Cost (GPU Days)	Comparable Search Space	Search Method
		Best	Average				
Shake-Shake	[16]	N/A	2.56	26.2	-	-	manual
PyramidNet	[50]	2.31	N/A	26	-	-	manual
NASNet-A*	[58]	N/A	2.65	3.3	2000	N	RL
AmoebaNet-B*	[43]	N/A	2.55 ± 0.05	2.8	3150	N	evolution
ProxylessNAS‡	[9]	2.08	N/A	5.7	4	N	gradient
ENAS	[40]	2.89	N/A	4.6	0.5	Y	RL
Random search WS†	[29]	2.71	2.85 ± 0.08	3.8	0.7	Y	random
ASNG-NAS	[3]	N/A	2.83 ± 0.14	3.9	0.1	Y	gradient
SNAS	[48]	N/A	2.85 ± 0.02	2.8	1.5	Y	gradient
DARTS (1st-order)†	[32]	N/A	3.00 ± 0.14	3.3	0.4	Y	gradient
DARTS (2nd-order)†	[32]	N/A	2.76 ± 0.09	3.3	1	Y	gradient
PDARTS#	[11]	2.50	N/A	3.4	0.3	Y	gradient
PC-DARTS†	[49]	N/A	2.57 ± 0.07	3.6	0.1	Y	gradient
GAEA PC-DARTS†	Ours	2.39	2.50 ± 0.06	3.7	0.1	Y	gradient

* We show results for networks with a comparable number of parameters.

† For fair comparison to other work, we show the search cost for training the shared-weights network with a single initialization.

‡ Search space and backbone architecture (PyramidNet) differ from the DARTS setting.

PDARTS results are not reported for multiple seeds. Additionally, PDARTS uses deeper weight-sharing networks during the search process, on which PC-DARTS has also been shown to improve performance [49]. We expect GAEA PC-DARTS to further improve if combined with PDARTS’s deeper weight-sharing networks.

Table 1: DARTS Benchmark (CIFAR-10): Comparison with manually designed networks and those found by SOTA NAS methods, mainly on the DARTS search space [32]. Results are grouped by the type of search method: manually designed, full-evaluation NAS, and weight-sharing NAS. All test errors are for models trained with auxiliary towers and cutout (parameter counts exclude auxiliary weights). Test errors we report are averaged over 10 seeds. “-” indicates that the field does not apply while “N/A” indicates unknown. Note that search cost is hardware-dependent; our results used Tesla V100 GPUs.

GAEA PC-DARTS on ImageNet We also evaluate GAEA PC-DARTS by searching directly on ImageNet. Here we follow the setup of [49] by using random subsamples containing 10% and 2.5% of the training images from ILSVRC2012 [44] as the training and validation sets, respectively. We fixed the architecture weights for the first 35 epochs before running GAEA PC-DARTS with a learning rate of 0.1. All other hyperparameters match those used by [49]. We depict the architecture found by GAEA PC-DARTS for ImageNet in Figure 3.

Table 2 shows the final evaluation performance of both the architecture found by GAEA PC-DARTS on CIFAR-10 as well as the one searched directly on ImageNet when trained from scratch for 250 epochs using the same hyperparameter settings as [49]. Our results demonstrate that the architecture found by GAEA PC-DARTS for ImageNet achieves a top-1 test error of 24.0%, which is state-of-the-art performance in the mobile setting on ImageNet when excluding additional training modifications like label smoothing [36], AutoAugment [12], Swish activation [42], and squeeze-and-excite modules [21]. Additionally, the architecture found by GAEA PC-DARTS for CIFAR-10 and transferred to ImageNet achieves a test error of 24.2%, which is comparable to the 24.2% error for

Architecture	Source	Test Error		Params (M)	Search Cost (GPU Days)	Search Method
		top-1	top-5			
MobileNet	[20]	29.4	10.5	4.2	-	manual
ShuffleNet V2 2x	[34]	25.1	N/A	~ 5	-	manual
NASNet-A*	[58]	26.0	8.4	5.3	1800	RL
AmoebaNet-C*	[43]	24.3	7.6	6.4	3150	evolution
DARTS [†]	[32]	26.7	8.7	4.7	4.0	gradient
SNAS	[48]	27.3	9.2	4.3	1.5	gradient
ProxylessNAS [‡]	[9]	24.9	7.5	7.1	8.3	gradient
PDARTS [#]	[11]	24.4	7.4	4.9	0.3	gradient
PC-DARTS (CIFAR-10) [†]	[49]	25.1	7.8	5.3	0.1	gradient
PC-DARTS (ImageNet) [†]	[49]	24.2	7.3	5.3	3.8	gradient
GAEA PC-DARTS (CIFAR-10) [†]	Ours	24.3	7.3	5.3	0.1	gradient
GAEA PC-DARTS (ImageNet) [†]	Ours	24.0	7.3	5.6	3.8	gradient

* We show results for networks with a comparable number of parameters.

[†] For fair comparison to other work, we show the search cost for training the shared-weights network with a single initialization.

[‡] Search space and backbone architecture (PyramidNet) differ from the DARTS setting.

[#] PDARTS uses deeper weight-sharing networks during the search process, on which PC-DARTS has also been shown to improve performance. We expect GAEA PC-DARTS to further improve if combined with PDARTS’s deeper weight-sharing networks.

Table 2: **DARTS Benchmark (ImageNet):** Comparison with manually designed networks and those found by SOTA NAS methods, mainly on the DARTS search space [32]. Results are grouped by the type of search method: manually designed, full-evaluation NAS, and weight-sharing NAS. All test errors are for models trained with auxiliary towers and cutout but no other modifications, e.g. label smoothing [36], AutoAugment [12], swish activation [42], squeeze and excite modules [21], etc. “-” indicates that the field does not apply while “N/A” indicates unknown. Note that search cost is hardware-dependent; our results used Tesla V100 GPUs.

the architecture found by PC-DARTS searched directly on ImageNet. We depict the top architectures found by GAEA PC-DARTS for CIFAR-10 and ImageNet in Figure 3 of the appendix.

5.2 GAEA on NAS-Bench-1Shot1

NAS-Bench-1Shot1 [55] considers a subset of NAS-Bench-101 [53] that allows the benchmarking of weight-sharing methods on three different search spaces over CIFAR-10. The search spaces differ in the number of nodes considered as well as the number of input edges per node, which jointly affects the search space size. Specifically, search space 1 has 2487 possible architectures, search space 2 has 3609 possible architectures, and search space 3 has 24066 possible architectures. For all three search spaces, a single operation from {3x3 convolution, 1x1 convolution, 3x3 max-pool} is applied to the sum of inputs to a node.

Of the weight-sharing methods benchmarked by [55], PC-DARTS achieves the best performance on 2 of the 3 search spaces. Therefore, we apply GAEA again to PC-DARTS to investigate the impact of a geometry-aware approach on these search spaces. Figure 1 shows that GAEA PC-DARTS consistently finds better

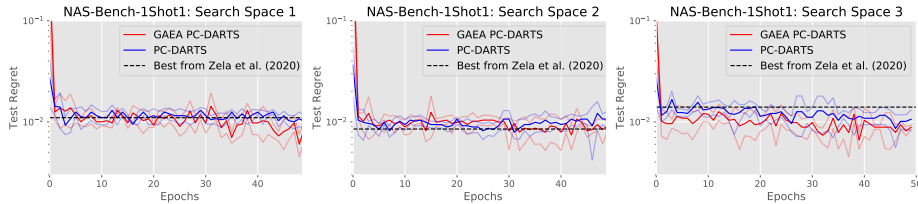


Fig. 1: **NAS-Bench-1Shot1**: Chart of the ground truth performance of the proposed architecture by epoch of shared-weights training averaged over 4 different shared-weights initializations. The dashed black line indicates the performance of the best weight-sharing method originally evaluated on the benchmark [55].

Method	Search (seconds)	CIFAR-10 test	CIFAR-100 test	ImageNet-16-120 test
RSPS	7587	87.66 ± 1.69	58.33 ± 4.34	31.14 ± 3.88
DARTS	35781	54.30 ± 0.00	15.61 ± 0.00	16.32 ± 0.00
SETN	34139	87.64 ± 0.00	59.05 ± 0.24	32.52 ± 0.21
GDAS	31609	93.61 ± 0.09	70.70 ± 0.30	41.71 ± 0.98
GDAS (reproduced)	27923 [†]	93.52 ± 0.15	67.52 ± 0.15	40.91 ± 0.12
GAEA GDAS	16754 [†]	93.55 ± 0.13	70.47 ± 0.47	40.91 ± 0.12
GAEA DARTS (ERM)	9061 [†]	94.10 ± 0.29	73.43 ± 0.13	46.36 ± 0.00
GAEA DARTS (bilevel)	7930 [†]	91.87 ± 0.57	71.87 ± 0.57	45.69 ± 0.56
REA	N/A	93.92 ± 0.30	71.84 ± 0.99	45.54 ± 1.03
RS	N/A	93.70 ± 0.36	71.04 ± 1.08	44.57 ± 1.25
REINFORCE	N/A	93.85 ± 0.37	71.71 ± 1.09	45.25 ± 1.18
BOHB	N/A	93.61 ± 0.52	70.85 ± 1.28	44.42 ± 1.49
ResNet	N/A	93.97	70.86	43.63
Optimal	N/A	94.37	73.51	47.31

[†] Search cost measured on NVIDIA P100 GPUs.

Table 3: **NAS-Bench-201**: Results are separated into those for weight-sharing methods (top) and those for traditional hyperparameter optimization methods.

architectures on average than PC-DARTS and thus exceeds the performance of the best method from [55] on 2 of the 3 search spaces. We hypothesize that the benefits of GAEA are limited on this benchmark due to the near-saturation of NAS methods on its search spaces. In particular, existing NAS methods already obtain within 1% test error of the top architecture in each space, while the standard deviations of the test error for the top architectures in each space when evaluated with different initializations are 0.37%, 0.23% and 0.19%, respectively.

5.3 GAEA on NAS-Bench-201

NAS-Bench-201 considers one search space—evaluated on CIFAR-10, CIFAR-100, and ImageNet-16-120 [44]—that includes 4-node architectures with an operation

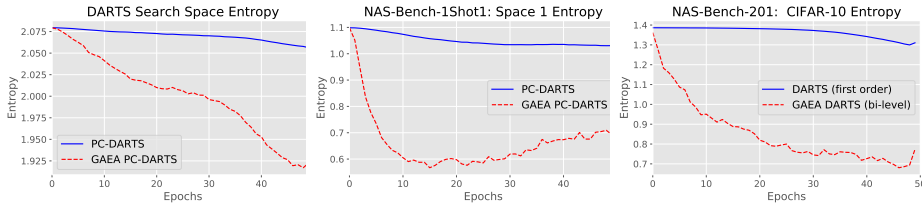


Fig. 2: **GAEA Convergence:** Evolution over search phase epochs of the average entropy of the operation-weights for GAEA and the approaches it modifies when run on the DARTS search space (left), NAS-Bench-1Shot1 Search Space 1 (middle), and NASBench-201 on CIFAR-10 (right). GAEA reduces entropy much more quickly than previous gradient-based methods, allowing it to quickly obtain sparse architecture weights. This leads to both faster convergence to a single architecture and a lower loss when pruning at the end of the search phase.

from $O = \{\text{none, skip connect, } 1 \times 1 \text{ convolution, } 3 \times 3 \text{ convolution, } 3 \times 3 \text{ avg pool}\}$ on each edge, yielding 15625 possible architectures. In Table 3 we report a subset of the results from [18] alongside our GAEA approaches, showing that GDAS [17] is the best previous weight-sharing method on all three datasets. Our reproduced results for GDAS are slightly worse than the published result on all three datasets but confirm GDAS as the top weight-sharing method. We evaluate GAEA GDAS on the three datasets and find that it achieves better results on CIFAR-100 than our reproduced runs of GDAS and similar results on the other two datasets.

However, as we are interested in improving upon the reported results as well, we proceeded to investigate the performance of GAEA when applied to first-order DARTS. We evaluated GAEA DARTS with both single-level (ERM) and bilevel optimization for architecture parameters; recall that in the bilevel case we optimize the architecture parameters w.r.t. the validation loss and the shared weights w.r.t. the training loss, whereas in the ERM approach there is no training-validation split. Our results show that GAEA DARTS (ERM) achieves state-of-the-art performance on all three datasets, exceeding the test accuracy of both weight-sharing and traditional hyperparameter optimization approaches by a wide margin. This result also shows that our convergence theory, which is for the single-level case, is useful to directly understand strong NAS methods. GAEA DARTS (bilevel) does not perform as well as single-level but still exceeds all other methods on CIFAR-100 and ImageNet-16-120.

5.4 Convergence of GAEA

While in the previous sections we focused on the test accuracy of GAEA, we now examine the impact of GAEA on the speed of convergence of the architecture parameters during training. Figure 2 shows the entropy of the operation weights averaged across nodes for a GAEA-variant versus the base method across all three benchmarks. It is evident that the entropy of operation weights decreases much

faster for GAEA-modified approaches across all benchmarks relative to the base methods. This also validates our expectation that GAEA encourages sparsity in architecture parameters, which should alleviate the mismatch between using a continuous relaxation of the architecture space and the discrete architecture derivation performed at the end of search. Note that, in addition to GAEA’s use of exponentiated gradient over the simplex, the entropy decrease of PC-DARTS may be further slowed by an additional weight decay term that is applied to architecture weights, which is not required for GAEA PC-DARTS.

6 Conclusion

This paper argues for a more principled, geometry-aware development process for gradient-based NAS with weight-sharing. In support of this, we develop provable optimization guarantees that allow us to reason formally about the convergence rate of successful algorithms such as ENAS [40] and DARTS [32]. Our analysis inspires GAEA, a simple modification of gradient-based NAS methods that attains state-of-the-art performance on several computer vision benchmarks while enjoying favorable speed and sparsity properties. We believe that obtaining high-performance NAS algorithms for wide variety of applications in computer vision and beyond will continue to require a similar co-design of search space parameterizations and optimization methods, and that our geometry-aware framework can help accelerate this development process.

Acknowledgments

We thank Jeremy Cohen, Jeffrey Li, and Nicholas Roberts for helpful feedback. This work was supported in part by DARPA FA875017C0141, National Science Foundation grants CCF-1535967, CCF-1910321, IIS-1618714, IIS-1705121, IIS-1838017, and IIS-1901403, a Microsoft Research Faculty Fellowship, a Bloomberg Data Science research grant, an Amazon Research Award, an Amazon Web Services Award, an Okawa Grant, a Google Faculty Award, a JP Morgan AI Research Faculty Award, and a Carnegie Bosch Institute Research Award. Any opinions, findings and conclusions, or recommendations expressed in this material are those of the authors and do not necessarily reflect the views of DARPA, the National Science Foundation, or any other funding agency.

Bibliography

- [1] Abernethy, J., Hazan, E., Rakhlin, A.: Competing in the dark: An efficient algorithm for bandit linear optimization. In: Proceedings of the International Conference on Computational Learning Theory (2008)
- [2] Ajanthan, T., Gupta, K., Torr, P.H.S., Hartley, R., Dokania, P.K.: Mirror descent view for neural network quantization (2019), arXiv
- [3] Akimoto, Y., Shirakawa, S., Noshinari, N., Uchida, K., Saito, S., Nishida, K.: Adaptive stochastic natural gradient method for one-shot neural architecture search. In: Proceedings of the 36th International Conference on Machine Learning (2019)
- [4] Arora, S., Hazan, E., Kale, S.: The multiplicative weights update method: a meta-algorithm and applications. *Theory of Computing* **8**, 121–164 (2012)
- [5] Beck, A.: *First-Order Methods in Optimization*. MOS-SIAM (2017)
- [6] Beck, A., Teboulle, M.: Mirror descent and nonlinear projected subgradient methods for convex optimization. *Operations Research Letters* **31**, 167–175 (2003)
- [7] Bregman, L.M.: The relaxation method of finding the common point of convex sets and its application to the solution of problems in convex programming. *USSR Computational Mathematics and Mathematical Physics* **7**, 200–217 (1967)
- [8] Bubeck, S., Cohen, M.B., Lee, J.R., Lee, Y.T., , Mądry, A.: K-server via multiscale entropic regularization. In: Proceedings of the 50th Annual ACM SIGACT Symposium on Theory of Computing (2018)
- [9] Cai, H., Zhu, L., Han, S.: ProxylessNAS: Direct neural architecture search on target task and hardware. In: Proceedings of the 7th International Conference on Learning Representations (2019)
- [10] Carlucci, F.M., Esperança, P.M., Singh, M., Yang, A., Gabillon, V., Xu, X., Chen, Z., Wang, J.: MANAS: Multi-agent neural architecture search (2019), arXiv
- [11] Chen, X., Xie, L., Wu, J., Tian, Q.: Progressive differentiable architecture search: Bridging the depth gap between search and evaluation. In: Proceedings of the IEEE International Conference on Computer Vision (2019)
- [12] Cubuk, E.D., Zoph, B., Mane, D., Vasudevan, V., Le, Q.V.: AutoAugment: Learning augmentation strategies from data. In: Proceedings of the IEEE Conference on Conference on Computer Vision and Pattern Recognition (2019)
- [13] Dang, C.D., Lan, G.: Stochastic block mirror descent methods for nonsmooth and stochastic optimization. *SIAM Journal on Optimization* **25**, 856–881 (2015)
- [14] Daskalakis, C., Ilyas, A., Syrgkanis, V., Zeng, H.: Training GANs with optimism. In: Proceedings of the 6th International Conference on Learning Representations (2018)

- [15] Davis, D., Drusvyatskiy, D.: Stochastic model-based minimization of weakly convex functions. *SIAM Journal on Optimization* **29**(1), 207–239 (2019)
- [16] DeVries, T., Taylor, G.W.: Improved regularization of convolutional neural networks with cutout (2017), arXiv
- [17] Dong, X., Yang, Y.: Searching for a robust neural architecture in four GPU hours. In: *Proceedings of the IEEE Conference on Computer Vision and Pattern Recognition* (2019)
- [18] Dong, X., Yang, Y.: NAS-Bench-201: Extending the scope of reproducible neural architecture search. In: *Proceedings of the 8th International Conference on Learning Representations* (2020)
- [19] Franceschi, L., Frasconi, P., Salzo, S., Grazzi, R., Pontil, M.: Bilevel programming for hyperparameter optimization and meta-learning. In: *Proceedings of the 35th International Conference on Machine Learning* (2018)
- [20] Howard, A.G., Zhu, M., Chen, B., Kalenichenko, D., Wang, W., Weyand, T., Andreetto, M., Adam, H.: MobileNets: Efficient convolutional neural networks for mobile vision applications (2017), arXiv
- [21] Hu, J., Shen, L., Sun, G.: Squeeze-and-excitation networks. In: *Proceedings of the IEEE Conference on Conference on Computer Vision and Pattern Recognition* (2018)
- [22] Hundt, A., Jain, V., Hager, G.D.: sharpDARTS: Faster and more accurate differentiable architecture search (2019), arXiv
- [23] Kingma, D.P., Ba, J.: Adam: A method for stochastic optimization. In: *Proceedings of the 3rd International Conference on Learning Representations* (2015)
- [24] Kleinberg, B., Li, Y., Yuan, Y.: An alternative view: When does SGD escape local minima? In: *Proceedings of the 35th International Conference on Machine Learning* (2018)
- [25] Krizhevksy, A.: Learning multiple layers of features from tiny images. Tech. rep. (2009)
- [26] Kunapuli, G., Shavlik, J.: Mirror descent for metric learning: A unified approach. In: *Proceedings of the Joint European Conference on Machine Learning and Knowledge Discovery in Databases* (2012)
- [27] Laube, K.A., Zell, A.: Prune and replace NAS. In: *Proceedings of the IEEE International Conference on Machine Learning and Applications* (2019)
- [28] Li, G., Zhang, X., Wang, Z., Li, Z., Zhang, T.: StacNAS: Towards stable and consistent differentiable neural architecture search (2019), arXiv
- [29] Li, L., Talwalkar, A.: Random search and reproducibility for neural architecture search. In: *Proceedings of the Conference on Uncertainty in Artificial Intelligence* (2019)
- [30] Liang, H., Zhang, S., Sun, J., He, X., Huang, W., Zhuang, K., Li, Z.: DARTS+: Improved differentiable architecture search with early stopping (2019), arXiv
- [31] Liu, C., Zoph, B., Neumann, M., Shlens, J., Hua, W., Li, L.J., Fei-Fei, L., Yuille, A., Huang, J., Murphy, K.: Progressive neural architecture search. In: *Proceedings of the European Conference on Computer Vision* (2018)

- [32] Liu, H., Simonyan, K., Yang, Y.: DARTS: Differentiable architecture search. In: Proceedings of the 7th International Conference on Learning Representations (2019)
- [33] Luong, D.V.N., Parpas, P., Rueckert, D., Rustem, B.: Solving MRF minimization by mirror descent. In: Advances in Visual Computing (2012)
- [34] Ma, N., Zhang, X., Zheng, H.T., Sun, J.: ShuffleNet V2: Practical guidelines for efficient CNN architecture design. In: Proceedings of the European Conference on Computer Vision (2018)
- [35] Mahadevan, S., Liu, B.: Sparse q-learning with mirror descent. In: Proceedings of the Conference on Uncertainty in Artificial Intelligence (2012)
- [36] Müller, R., Kornblith, S., Hinton, G.E.: When does label smoothing help? In: Advances in Neural Information Processing Systems (2019)
- [37] Nayman, N., Noy, A., Ridnik, T., Friedman, I., Jin, R., Zelnik-Manor, L.: XNAS: Neural architecture search with expert advice. In: Advances in Neural Information Processing Systems (2019)
- [38] Nemirovski, A., Yudin, D.: Problem Complexity and Method Efficiency in Optimization. Wiley (1983)
- [39] Noy, A., Nayman, N., Ridnik, T., Doveh, S., Friedman, I., Giryas, R., Zelnik-Manor, L.: ASAP: Architecture search, anneal and prune (2019), arXiv
- [40] Pham, H., Guan, M.Y., Zoph, B., Le, Q.V., Dean, J.: Efficient neural architecture search via parameter sharing. In: Proceedings of the 35th International Conference on Machine Learning (2018)
- [41] Rakhlin, A., Sridharan, K.: Optimization, learning, and games with predictable sequences. In: Advances in Neural Information Processing Systems (2013)
- [42] Ramachandran, P., Zoph, B., Le, Q.V.: Searching for activation functions (2017), arXiv
- [43] Real, E., Aggarwal, A., Huang, Y., Le, Q.V.: Regularized evolution for image classifier architecture search. In: Proceedings of the 33rd AAAI Conference on Artificial Intelligence (2019)
- [44] Russakovsky, O., Deng, J., Su, H., Krause, J., Satheesh, S., Ma, S., Huang, Z., Karpathy, A., Khosla, A., Bernstein, M., Berg, A.C., Fei-Fei, L.: ImageNet large scale visual recognition challenge. *International Journal of Computer Vision* **115**(3), 211–252 (2015)
- [45] Shalev-Shwartz, S.: Online learning and online convex optimization. *Foundations and Trends in Machine Learning* **4**(2), 107—194 (2011)
- [46] Strubell, E., Ganesh, A., McCallum, A.: Energy and policy considerations for deep learning in NLP. In: Proceedings of the 57th Conference of the Association for Computational Linguistics (2019)
- [47] Wilson, A.C., Roelofs, R., Stern, M., Srebro, N., Recht, B.: The marginal value of adaptive gradient methods in machine learning. In: Advances in Neural Information Processing Systems (2017)
- [48] Xie, S., Zheng, H., Liu, C., Lin, L.: SNAS: Stochastic neural architecture search. In: Proceedings of the 7th International Conference on Learning Representations (2019)

- [49] Xu, Y., Xie, L., Zhang, X., Chen, X., Qi, G.J., Tian, Q., Xiong, H.: PC-DARTS: Partial channel connections for memory-efficient architecture search. In: Proceedings of the 8th International Conference on Learning Representations (2020)
- [50] Yamada, Y., Iawmura, M., Kise, K.: ShakeDrop regularization (2018), arXiv
- [51] Yang, Z., Wang, Y., Chen, X., Shi, B., Xu, C., Xu, C., Tian, Q., Xu, C.: CARS: Continuous evolution for efficient neural architecture search. In: Proceedings of the IEEE Conference on Computer Vision and Pattern Recognition (2020)
- [52] Yao, Q., Xu, J., Tu, W.W., Zhu, Z.: Efficient neural architecture search via proximal iterations. In: Proceedings of the 34th AAAI Conference on Artificial Intelligence (2020)
- [53] Ying, C., Klein, A., Christiansen, E., Real, E., Murphy, K., Hutter, F.: NAS-Bench-101: Towards reproducible neural architecture search. In: Proceedings of the 36th International Conference on Machine Learning (2019)
- [54] Zela, A., Elsken, T., Saikia, T., Marrakchi, Y., Brox, T., Hutter, F.: Understanding and robustifying differentiable architecture search. In: Proceedings of the 8th International Conference on Learning Representations (2020)
- [55] Zela, A., Siems, J., Hutter, F.: NAS-Bench-1Shot1: Benchmarking and dissecting one-shot neural architecture search. In: Proceedings of the 8th International Conference on Learning Representations (2020)
- [56] Zhang, S., He, N.: On the convergence rate of stochastic mirror descent for nonsmooth nonconvex optimization (2018), arXiv
- [57] Zheng, X., Ji, R., Tang, L., Zhang, B., Liu, J., Tian, Q.: Multinomial distribution learning for effective neural architecture search. In: Proceedings of the IEEE International Conference on Computer Vision (2019)
- [58] Zoph, B., Vasudevan, V., Shlens, J., Le, Q.V.: Learning transferable architectures for scalable image recognition. In: Proceedings of the IEEE Conference on Computer Vision and Pattern Recognition (2018)

A Optimization

This section contains proofs and generalizations of the non-convex optimization results in Section 3. Throughout this section, \mathbb{V} denotes a finite-dimensional real vector space with Euclidean inner product $\langle \cdot, \cdot \rangle$, \mathbb{R}_+ denotes the set of nonnegative real numbers, and $\overline{\mathbb{R}}$ denotes the set of extended real numbers $\mathbb{R} \cup \{\pm\infty\}$.

A.1 Preliminaries

Definition 1 Consider a closed and convex subset $\mathcal{X} \subset \mathbb{V}$. For any $\alpha > 0$ and norm $\|\cdot\| : \mathcal{X} \mapsto \mathbb{R}_+$ an everywhere-subdifferentiable function $f : \mathcal{X} \mapsto \overline{\mathbb{R}}$ is called **α -strongly-convex** w.r.t. $\|\cdot\|$ if $\forall \mathbf{x}, \mathbf{y} \in \mathcal{X}$ we have

$$f(\mathbf{y}) \geq f(\mathbf{x}) + \langle \nabla f(\mathbf{x}), \mathbf{y} - \mathbf{x} \rangle + \frac{\alpha}{2} \|\mathbf{y} - \mathbf{x}\|^2$$

Definition 2 Consider a closed and convex subset $\mathcal{X} \subset \mathbb{V}$. For any $\beta > 0$ and norm $\|\cdot\| : \mathcal{X} \mapsto \mathbb{R}_+$ an continuously-differentiable function $f : \mathcal{X} \mapsto \mathbb{R}$ is called **β -strongly-smooth** w.r.t. $\|\cdot\|$ if $\forall \mathbf{x}, \mathbf{y} \in \mathcal{X}$ we have

$$f(\mathbf{y}) \leq f(\mathbf{x}) + \langle \nabla f(\mathbf{x}), \mathbf{y} - \mathbf{x} \rangle + \frac{\beta}{2} \|\mathbf{y} - \mathbf{x}\|^2$$

Definition 3 Let \mathcal{X} be a closed and convex subset of \mathbb{V} . The **Bregman divergence** induced by a strictly convex, continuously-differentiable **distance-generating function (DGF)** $\phi : \mathcal{X} \mapsto \overline{\mathbb{R}}$ is

$$D_\phi(\mathbf{x}|\mathbf{y}) = \phi(\mathbf{x}) - \phi(\mathbf{y}) - \langle \nabla \phi(\mathbf{y}), \mathbf{x} - \mathbf{y} \rangle \quad \forall \mathbf{x}, \mathbf{y} \in \mathcal{X}$$

By definition, the Bregman divergence satisfies the following properties:

1. $D_\phi(\mathbf{x}|\mathbf{y}) \geq 0 \quad \forall x, y \in \mathcal{X}$ and $D_\phi(\mathbf{x}|\mathbf{y}) = 0 \iff x = y$.
2. If ϕ is α -strongly-convex w.r.t. norm $\|\cdot\|$ then so is $D_\phi(\cdot|\mathbf{y}) \quad \forall \mathbf{y} \in \mathcal{X}$.
Furthermore, $D_\phi(\mathbf{x}|\mathbf{y}) \geq \frac{\alpha}{2} \|\mathbf{x} - \mathbf{y}\|^2 \quad \forall \mathbf{x}, \mathbf{y} \in \mathcal{X}$.
3. If ϕ is β -strongly-smooth w.r.t. norm $\|\cdot\|$ then so is $D_\phi(\cdot|\mathbf{y}) \quad \forall \mathbf{y} \in \mathcal{X}$.
Furthermore, $D_\phi(\mathbf{x}|\mathbf{y}) \leq \frac{\beta}{2} \|\mathbf{x} - \mathbf{y}\|^2 \quad \forall \mathbf{x}, \mathbf{y} \in \mathcal{X}$.

Definition 4 [56, Definition 2.1] Consider a closed and convex subset $\mathcal{X} \subset \mathbb{V}$. For any $\gamma > 0$ and $\phi : \mathcal{X} \mapsto \overline{\mathbb{R}}$ an everywhere-subdifferentiable function $f : \mathcal{X} \mapsto \mathbb{R}$ is called **γ -relatively-weakly-convex (γ -RWC)** w.r.t. ϕ if $f(\cdot) + \gamma\phi(\cdot)$ is convex on \mathcal{X} .

Definition 5 [56, Definition 2.3] Consider a closed and convex subset $\mathcal{X} \subset \mathbb{V}$. For any $\lambda > 0$, function $f : \mathcal{X} \mapsto \mathbb{R}$, and DGF $\phi : \mathcal{X} \mapsto \overline{\mathbb{R}}$ the **Bregman proximal operator** of f is

$$\text{prox}_\lambda(\mathbf{x}) = \arg \min_{\mathbf{u} \in \mathcal{X}} \lambda f(\mathbf{u}) + D_\phi(\mathbf{u}|\mathbf{x})$$

Definition 6 [56, Equation 2.11] Consider a closed and convex subset $\mathcal{X} \subset \mathbb{V}$. For any $\lambda > 0$, function $f : \mathcal{X} \mapsto \mathbb{R}$, and DGF $\phi : \mathcal{X} \mapsto \overline{\mathbb{R}}$ the **Bregman stationarity** of f at any point $\mathbf{x} \in \mathcal{X}$ is

$$\Delta_\lambda(\mathbf{x}) = \frac{D_\phi(\mathbf{x}|\text{prox}_\lambda(\mathbf{x})) + D_\phi(\text{prox}_\lambda(\mathbf{x})|\mathbf{x})}{\lambda^2}$$

A.2 Results

Throughout this subsection let $\mathbb{V} = \times_{i=1}^b \mathbb{V}_i$ be a product space of b finite-dimensional real vector spaces \mathbb{V}_i , each with an associated norm $\|\cdot\|_i : \mathbb{V}_i \mapsto \mathbb{R}_+$, and $\mathcal{X} = \times_{i=1}^b \mathcal{X}_i$ be a product set of b subsets $\mathcal{X}_i \subset \mathbb{V}_i$, each with an associated 1-strongly-convex DGF $\phi_i : \mathcal{X}_i \mapsto \overline{\mathbb{R}}$ w.r.t. $\|\cdot\|_i$. For each $i \in [b]$ will use $\|\cdot\|_{i,*}$ to denote the dual norm of $\|\cdot\|_i$ and for any element $\mathbf{x} \in \mathcal{X}$ we will use \mathbf{x}_i to denote its component in block i and \mathbf{x}_{-i} to denote the component across all blocks other than i . Define the functions $\|\cdot\| : \mathbb{V} \mapsto \mathbb{R}_+$ and $\|\cdot\|_* \mathbb{V} \mapsto \mathbb{R}_+$ for any $\mathbf{x} \in \mathbb{V}$ by $\|\mathbf{x}\|^2 = \sum_{i=1}^b \|\mathbf{x}_i\|_i^2$ and $\|\mathbf{x}\|_*^2 = \sum_{i=1}^b \|\mathbf{x}_i\|_{i,*}^2$, respectively, and the function $\phi : \mathcal{X} \mapsto \overline{\mathbb{R}}$ for any $\mathbf{x} \in \mathcal{X}$ by $\phi(\mathbf{x}) = \sum_{i=1}^b \phi_i(\mathbf{x}_i)$. Finally, for any $n \in \mathbb{N}$ we will use $[n]$ to denote the set $\{1, \dots, n\}$.

Setting 1 For some fixed constants $\gamma_i, L_i > 0$ for each $i \in [b]$ we have the following:

1. $f : \mathcal{X} \mapsto \mathbb{R}$ is everywhere-subdifferentiable with minimum $f^* > -\infty$ and for all $\mathbf{x} \in \mathcal{X}$ and each $i \in [b]$ the restriction $f(\cdot, \mathbf{x}_{-i})$ is γ_i -RWC w.r.t. ϕ_i .
2. For each $i \in [b]$ there exists a stochastic oracle G_i that for input $\mathbf{x} \in \mathcal{X}$ outputs a random vector $G_i(\mathbf{x}, \xi)$ s.t. $\mathbb{E}_\xi G_i(\mathbf{x}, \xi) \in \partial_i f(\mathbf{x})$, where $\partial_i f(\mathbf{x})$ is the subdifferential set of the restriction $f(\cdot, \mathbf{x}_{-i})$ at \mathbf{x}_i . Moreover, $\mathbb{E}_\xi \|G_i(\mathbf{x}, \xi)\|_{i,*}^2 \leq L_i^2$.

Define $\gamma = \max_{i \in [b]} \gamma_i$ and $L^2 = \sum_{i=1}^b L_i^2$.

Claim 1 $\|\cdot\|$ is a norm on \mathbb{V} .

Proof. Positivity and homogeneity are trivial. For the triangle inequality, note that for any $\lambda \in [0, 1]$ and any $\mathbf{x}, \mathbf{y} \in \mathcal{X}$ we have that

$$\begin{aligned} \|\lambda \mathbf{x} + (1 - \lambda) \mathbf{y}\| &= \sqrt{\sum_{i=1}^b \|\lambda \mathbf{x}_i + (1 - \lambda) \mathbf{y}_i\|_i^2} \\ &\leq \sqrt{\sum_{i=1}^b (\lambda \|\mathbf{x}_i\|_i + (1 - \lambda) \|\mathbf{y}_i\|_i)^2} \\ &\leq \lambda \sqrt{\sum_{i=1}^b \|\mathbf{x}_i\|_i^2} + (1 - \lambda) \sqrt{\sum_{i=1}^b \|\mathbf{y}_i\|_i^2} \\ &= \lambda \|\mathbf{x}\| + (1 - \lambda) \|\mathbf{y}\| \end{aligned}$$

where the first inequality follows by convexity of the norms $\|\cdot\|_i \forall i \in [b]$ and the fact that the Euclidean norm on \mathbb{R}^b is nondecreasing in each argument, while the second inequality follows by convexity of the Euclidean norm on \mathbb{R}^b . Setting $\lambda = \frac{1}{2}$ and multiplying both sides by 2 yields the triangle inequality.

Algorithm 2: Block-stochastic mirror descent over $\mathcal{X} = \times_{i=1}^b \mathcal{X}_i$ given associated DGFs $\phi_i : \mathcal{X}_i \mapsto \overline{\mathbb{R}}$.

Input: initialization $\mathbf{x}^{(1)} \in \mathcal{X}$, number of steps $T \geq 1$, step-size sequence $\{\eta_t\}_{t=1}^T$
for iteration $t \in [T]$ **do**
 sample $i \sim \text{Unif}[b]$
 set $\mathbf{x}_{-i}^{(t+1)} = \mathbf{x}_{-i}^{(t)}$
 get $\mathbf{g} = G_i(\mathbf{x}^{(t)}, \xi_t)$
 set $\mathbf{x}_i^{(t+1)} = \arg \min_{\mathbf{u} \in \mathcal{X}_i} \eta_t \langle \mathbf{g}, \mathbf{u} \rangle + D_{\phi_i}(\mathbf{u} \| \mathbf{x}_i^{(t)})$
Output: $\hat{\mathbf{x}} = \mathbf{x}^{(t)}$ w.p. $\frac{\eta_t}{\sum_{t=1}^T \eta_t}$.

Claim 2 $\frac{1}{2} \|\cdot\|_*^2$ is the convex conjugate of $\frac{1}{2} \|\cdot\|^2$.

Proof. Consider any $\mathbf{u} \in \mathbb{V}$. To upper-bound the convex conjugate note that

$$\begin{aligned} \sup_{\mathbf{x} \in \mathbb{V}} \langle \mathbf{u}, \mathbf{x} \rangle - \frac{\|\mathbf{x}\|^2}{2} &= \sup_{\mathbf{x} \in \mathbb{V}} \sum_{i=1}^b \langle \mathbf{u}_i, \mathbf{x}_i \rangle - \frac{\|\mathbf{x}_i\|_i^2}{2} \\ &\leq \sup_{\mathbf{x} \in \mathbb{V}} \sum_{i=1}^b \|\mathbf{u}_i\|_{i,*} \|\mathbf{x}_i\|_i - \frac{\|\mathbf{x}_i\|_i^2}{2} \\ &= \frac{1}{2} \sum_{i=1}^b \|\mathbf{u}_i\|_{i,*}^2 \\ &= \frac{\|\mathbf{u}\|_*^2}{2} \end{aligned}$$

where the first inequality follows by definition of a dual norm and the second by maximizing each term w.r.t. $\|\mathbf{x}_i\|_i$. For the lower bound, pick $\mathbf{x} \in \mathbb{V}$ s.t. $\langle \mathbf{u}_i, \mathbf{x}_i \rangle = \|\mathbf{u}_i\|_{i,*} \|\mathbf{x}_i\|_i$ and $\|\mathbf{x}_i\|_i = \|\mathbf{u}_i\|_{i,*} \forall i \in [b]$, which must exist by the definition of a dual norm. Then

$$\langle \mathbf{u}, \mathbf{x} \rangle - \frac{\|\mathbf{x}\|^2}{2} = \sum_{i=1}^b \langle \mathbf{u}_i, \mathbf{x}_i \rangle - \frac{\|\mathbf{x}_i\|_i^2}{2} = \frac{1}{2} \sum_{i=1}^b \frac{\|\mathbf{u}_i\|_{i,*}^2}{2} = \frac{\|\mathbf{u}\|_*^2}{2}$$

so $\sup_{\mathbf{x} \in \mathbb{V}} \langle \mathbf{u}, \mathbf{x} \rangle - \frac{1}{2} \|\mathbf{x}\|^2 \geq \frac{1}{2} \|\mathbf{u}\|_*^2$, completing the proof.

Theorem 2 *Let $\hat{\mathbf{x}}$ be the output of Algorithm 2 after T iterations with non-increasing step-size sequence $\{\eta_t\}_{t=1}^T$. Then under Setting 1, for any $\hat{\gamma} > \gamma$ we have that*

$$\mathbb{E}\Delta_{\frac{1}{\hat{\gamma}}}(\hat{\mathbf{x}}) \leq \frac{\hat{\gamma}b}{\hat{\gamma} - \gamma} \frac{\min_{\mathbf{u} \in \mathcal{X}} f(\mathbf{u}) + \hat{\gamma}D_\phi(\mathbf{u}|\|\mathbf{x}^{(1)}) - f^* + \frac{\hat{\gamma}L^2}{2b} \sum_{t=1}^T \eta_t^2}{\sum_{t=1}^T \eta_t}$$

where the expectation is w.r.t. ξ_t and the randomness of the algorithm.

Proof. Define transforms $\mathbf{U}_i, i \in [b]$ s.t. $\mathbf{U}_i^T \mathbf{x} = \mathbf{x}_i$ and $\mathbf{x} = \sum_{i=1}^b \mathbf{U}_i \mathbf{x}_i \forall \mathbf{x} \in \mathcal{X}$. Let G be a stochastic oracle that for input $\mathbf{x} \in \mathcal{X}$ outputs $G(\mathbf{x}, i, \xi) = b\mathbf{U}_i G_i(\mathbf{x}, \xi)$. This implies $\mathbb{E}_{i, \xi} G(\mathbf{x}, i, \xi) = \frac{1}{b} \sum_{i=1}^b b\mathbf{U}_i \mathbb{E}_\xi G_i(\mathbf{x}, \xi) \in \sum_{i=1}^b \mathbf{U}_i \partial_i f(\mathbf{x}) = \partial f(\mathbf{x})$ and $\mathbb{E}_{i, \xi} \|G(\mathbf{x}, i, \xi)\|_*^2 = \frac{1}{b} \sum_{i=1}^b b^2 \mathbb{E}_\xi \|\mathbf{U}_i G_i(\mathbf{x}, \xi)\|_{i,*}^2 \leq b \sum_{i=1}^b L_i^2 = bL^2$. Then

$$\begin{aligned} \mathbf{x}^{(t+1)} &= \mathbf{U}_i \left[\arg \min_{\mathbf{u} \in \mathcal{X}_i} \eta_t \langle g, \mathbf{u} \rangle + D_{\phi_i}(\mathbf{u}|\|\mathbf{x}_i^{(t)}) \right] \\ &= \mathbf{U}_i \mathbf{U}_i^T \left[\arg \min_{\mathbf{u} \in \mathcal{X}} \eta_t \langle \mathbf{U}_i G_i(\mathbf{x}^{(t)}, \xi_t), \mathbf{u} \rangle + \sum_{i=1}^b D_{\phi_i}(\mathbf{u}_i|\|\mathbf{x}_i^{(t)}) \right] \\ &= \arg \min_{\mathbf{u} \in \mathcal{X}} \frac{\eta_t}{b} \langle G(\mathbf{x}, i, \xi_t), \mathbf{u} \rangle + D_\phi(\mathbf{u}|\|\mathbf{x}^{(t)}) \end{aligned}$$

Thus Algorithm 2 is equivalent to [56, Algorithm 1] with stochastic oracle $G(\mathbf{x}, i, \xi)$, step-size sequence $\{\eta_t/b\}_{t=1}^T$, and no regularizer. Note that ϕ is 1-strongly-convex w.r.t. $\|\cdot\|$ and f is γ -RWC w.r.t. ϕ , so in light of Claims 1 and 2 our setup satisfies [56, Assumption 3.1]. The result then follows from [56, Theorem 3.1].

Corollary 1 *Under Setting 1 let $\hat{\mathbf{x}}$ be the output of Algorithm 2 with constant step-size $\eta_t = \sqrt{\frac{2b(f^{(1)} - f^*)}{\gamma L^2 T}} \forall t \in [T]$, where $f^{(1)} = f(\mathbf{x}^{(1)})$. Then we have*

$$\mathbb{E}\Delta_{\frac{1}{2\gamma}}(\hat{\mathbf{x}}) \leq 2L \sqrt{\frac{2b\gamma(f^{(1)} - f^*)}{T}}$$

where the expectation is w.r.t. ξ_t and the randomness of the algorithm. Equivalently, we can reach a point $\hat{\mathbf{x}}$ satisfying $\mathbb{E}\Delta_{\frac{1}{2\gamma}}(\hat{\mathbf{x}}) \leq \varepsilon$ in $\frac{8\gamma b L^2 (f^{(1)} - f^*)}{\varepsilon^2}$ stochastic oracle calls.

B Experiment Details

We provide additional detail on the experimental setup and hyperparameter settings used for each benchmark studied in Section 5. We also provide a more detailed discussion of how XNAS differs from GAEA, along with empirical results for XNAS on the NAS-Bench-201 benchmark.

B.1 DARTS Search Space

We consider the same search space as DARTS [32], which has become one of the standard search spaces for CNN cell search [37, 39, 30]. Following the evaluation procedure used in [32] and [49], our evaluation of GAEA PC-DARTS consists of three stages:

- **Stage 1:** In the search phase, we run GAEA PC-DARTS with 5 random seeds to reduce variance from different initialization of the shared-weights network.⁷
- **Stage 2:** We evaluate the best architecture identified by each search run by training from scratch.
- **Stage 3:** We perform a more thorough evaluation of the best architecture from stage 2 by training with ten different random seed initializations.

For completeness, we describe the convolutional neural network search space considered. A cell consists of 2 input nodes and 4 intermediate nodes for a total of 6 nodes. The nodes are ordered and subsequent nodes can receive the output of prior nodes as input so for a given node k , there are $k - 1$ possible input edges to node k . Therefore, there are a total of $2 + 3 + 4 + 5 = 14$ edges in the weight-sharing network.

An architecture is defined by selecting 2 input edges per intermediate node and also selecting a single operation per edge from the following 8 operations: (1) 3×3 separable convolution, (2) 5×5 separable convolution, (3) 3×3 dilated convolution, (4) 5×5 dilated convolution, (5) max pooling, (6) average pooling, (7) identity (8) zero. We use the same search space to design a “normal” cell and a “reduction” cell; the normal cells have stride 1 operations that do not change the dimension of the input, while the reduction cells have stride 2 operations that half the length and width dimensions of the input. In the experiments, for both cell types, , after which the output of all intermediate nodes are concatenated to form the output of the cell.

Stage 1: Architecture Search For stage 1, as is done by DARTS and PC-DARTS, we use GAEA PC-DARTS to update architecture parameters for a smaller shared-weights network in the search phase with 8 layers and 16 initial channels. All hyperparameters for training the weight-sharing network are the same as that used by PC-DARTS:

⁷ Note [32] trains the weight-sharing network with 4 random seeds. However, since PC-DARTS is significantly faster than DARTS, the cost of an additional seed is negligible.

```

train:
  scheduler: cosine
  lr_anneal_cycles: 1
  smooth_cross_entropy: false
  batch_size: 256
  learning_rate: 0.1
  learning_rate_min: 0.0
  momentum: 0.9
  weight_decay: 0.0003
  init_channels: 16
  layers: 8
  autoaugment: false
  cutout: false
  auxiliary: false
  drop_path_prob: 0
  grad_clip: 5

```

For GAEA PC-DARTS, we initialize the architecture parameters with equal weight across all options (equal weight across all operations per edge and equal weight across all input edges per node). Then, we train the shared-weights network for 10 epochs without performing any architecture updates to warmup the weights. Then, we use a learning rate of 0.1 for the exponentiated gradient update for GAEA PC-DARTS.

Stage 2 and 3: Architecture Evaluation For stages 2 and 3, we train each architecture for 600 epochs with the same hyperparameter settings as PC-DARTS:

```

train:
  scheduler: cosine
  lr_anneal_cycles: 1
  smooth_cross_entropy: false
  batch_size: 128
  learning_rate: 0.025
  learning_rate_min: 0.0
  momentum: 0.9
  weight_decay: 0.0003
  init_channels: 36
  layers: 20
  autoaugment: false
  cutout: true
  cutout_length: 16
  auxiliary: true
  auxiliary_weight: 0.4
  drop_path_prob: 0.3
  grad_clip: 5

```

Broad Reproducibility Our ‘broad reproducibility’ results in Table 4 show the final stage 3 evaluation performance of GAEA PC-DARTS for 2 additional sets of random seeds from stage 1 search. The performance of GAEA PC-DARTS for one set is similar to that reported in Table 1, while the other is on par with the performance reported for PC-DARTS in [49]. We do observe non-negligible variance in the performance of the architecture found by different random seed initializations of the shared-weights network, necessitating running multiple searches before selecting an architecture. We also found that it was possible to identify and eliminate poor performing architectures in just 20 epochs of training during stage 2 intermediate evaluation, thereby reducing the total training cost by over 75% (we only trained 3 out of 10 architectures for the entire 600 epochs).

Stage 3 Evaluation		
Set 1 (Reported)	Set 2	Set 3
2.50 ± 0.07	2.50 ± 0.09	2.60 ± 0.09

Table 4: GAEA PC-DARTS Stage 3 Evaluation for 3 sets of random seeds.

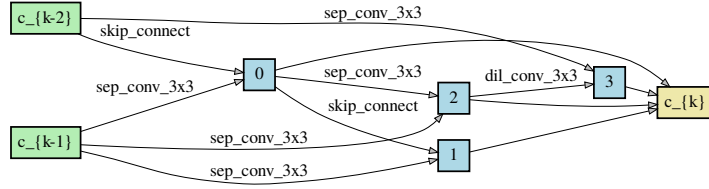
We depict the top architectures found by GAEA PC-DARTS for CIFAR-10 and ImageNet in Figure 3.

B.2 NAS-Bench-1Shot1

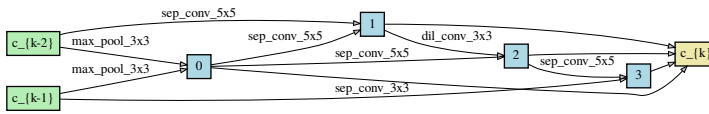
The NAS-Bench-1Shot1 benchmark [55] contains 3 different search spaces that are subsets of the NAS-Bench-101 search space. The search spaces differ in the number of nodes and the number of input edges selected per node. We refer the reader to [55] for details about each individual search space.

Of the NAS methods evaluated in [55], PC-DARTS had the most robust performance across the three search spaces and converged to the best architecture in search spaces 1 and 3. GDAS, a probabilistic gradient NAS method, achieved the best performance on search space 2. Hence, we focused on applying a geometry-aware approach to PC-DARTS. We implemented GAEA PC-DARTS within the repository provided by the authors of [55] available at <https://github.com/automl/nasbench-1shot1>. We used the same hyperparameter settings for training the weight-sharing network as that used by [55] for PC-DARTS. Similar to the previous benchmark, we initialize architecture parameters to allocate equal weight to all options. For the architecture updates, the only hyperparameter for GAEA PC-DARTS is the learning rate for exponentiated gradient, which we set to 0.1.

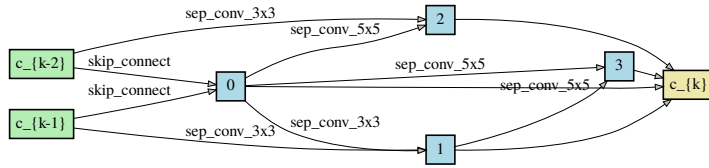
As mentioned in Section 5, the search spaces considered in this benchmark differ in that operations are applied after aggregating all edge inputs to a node instead of per edge input as in the DARTS and NAS-Bench-201 search spaces. This structure inherently limits the size of the weight-sharing network to scale with the number of nodes instead of the number of edges ($\mathcal{O}(|\text{nodes}|^2)$),



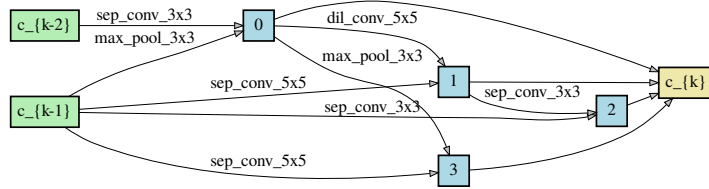
(a) CIFAR-10: Normal Cell



(b) CIFAR-10: Reduction Cell



(c) ImageNet: Normal Cell



(d) ImageNet: Reduction Cell

Fig. 3: The best normal and reduction cells found by GAEA PC-DARTS on CIFAR-10 (top) and ImageNet (bottom).

thereby limiting the degree of overparameterization. Understanding the impact of overparameterization on the performance of weight-sharing NAS methods is a direction for future study.

B.3 NAS-Bench-201

The NAS-Bench-201 benchmark [18] evaluates a single search space across 3 datasets: CIFAR-10, CIFAR-100, and a miniature version of ImageNet (ImageNet-16-120). ImageNet-16-120 is a downsampled version of ImageNet with 16×16 images and 120 classes for a total of 151.7k training images, 3k validation images, and 3k test images.

The authors of [18] evaluated the architecture search performance of multiple weight-sharing methods and traditional hyperparameter optimization methods on all three datasets. According to the results from [18], GDAS outperformed other weight-sharing methods by a large margin. Hence, we first evaluated the performance of GAEA GDAS on each of the three datasets. Our implementation of GAEA GDAS uses an architecture learning rate of 0.1, which matches the learning rate used for GAEA approaches in the previous two benchmarks. Additionally, we run GAEA GDAS for 150 epochs instead of 250 epochs used for GDAS in the original benchmarked results; this is why the search cost is lower for GAEA GDAS. All other hyperparameter settings are the same. Our results for GAEA GDAS is comparable to the reported results for GDAS on CIFAR-10 and CIFAR-100 but slightly lower on ImageNet-16-120. Compared to our reproduced results for GDAS, GAEA GDAS outperforms GDAS on CIFAR-100 and matches it on CIFAR-10 and ImageNet-16-120.

Next, to see if we can use GAEA to further improve the performance of weight-sharing methods, we evaluated GAEA DARTS (first order) applied to both the single-level (ERM) and bi-level optimization problems. Again, we used a learning rate of 0.1 and trained GAEA DARTS for 25 epochs on each dataset. The one additional modification we made was to exclude the **zero** operation, which limits GAEA DARTS to a subset of the search space. To isolate the impact of this modification, we also evaluated first-order DARTS with this modification. Similar to [18], we observe DARTS with this modification to also converge to architectures with nearly all skip connections, resulting in similar performance as that reported in [18]. We present the learning curves of the oracle architecture recommended by DARTS and GAEA DARTS (when excluding zero operation) over the training horizon for 4 different runs in Figure 4. For GAEA GDAS and GAEA DARTS, we train the weight-sharing network with the following hyperparameters:

```
train:
  scheduler: cosine
  lr_anneal_cycles: 1
  smooth_cross_entropy: false
  batch_size: 64
  learning_rate: 0.025
```

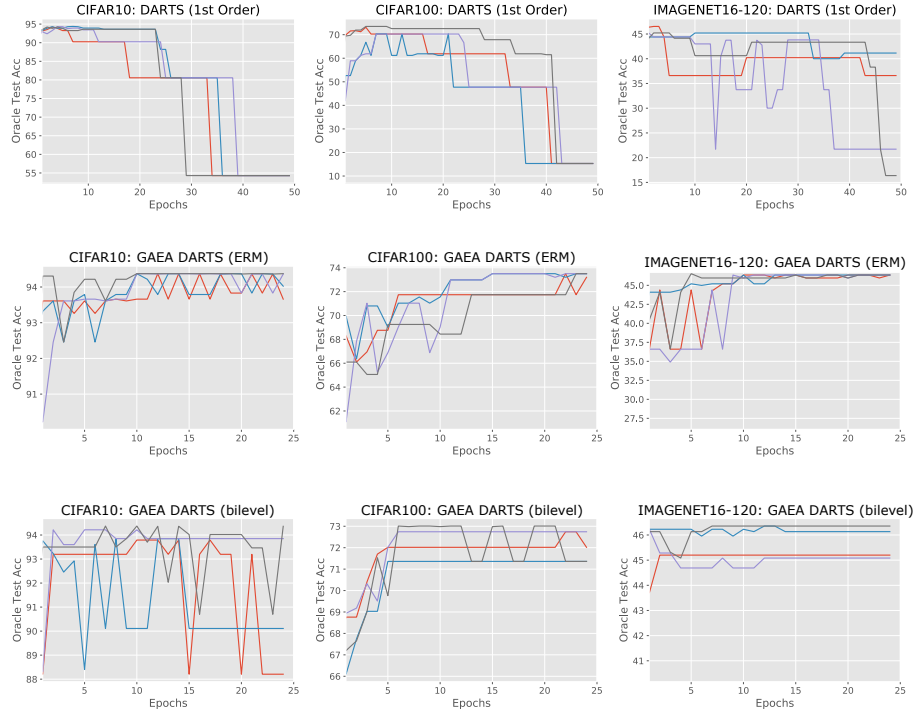


Fig. 4: **NAS-Bench-201: Learning Curves.** Evolution over search phase epochs of the best architecture according to the NAS method. DARTS (first-order) converges to nearly all skip connections while GAEA is able to suppress overfitting to the mixture relaxation by encouraging sparsity in operation weights.

```

learning_rate_min: 0.001
momentum: 0.9
weight_decay: 0.0003
init_channels: 16
layers: 5
autoaugment: false
cutout: false
auxiliary: false
auxiliary_weight: 0.4
drop_path_prob: 0
grad_clip: 5

```

Surprisingly, we observe single-level optimization to yield better performance than solving the bi-level problem with GAEA DARTS on this search space. In fact, the performance of GAEA DARTS (ERM) not only exceeds that of GDAS, but also outperforms traditional hyperparameter optimization approaches on all three datasets, nearly reaching the optimal accuracy on all three datasets.

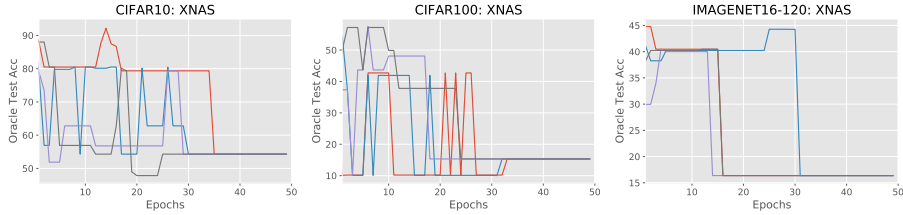


Fig. 5: **NAS-Bench-201: XNAS Learning Curves.** Evolution over search phase epochs of the best architecture according 4 runs of XNAS. XNAS exhibits the same behavior as DARTS and converges to nearly all skip connections.

In contrast, GAEA DARTS (bi-level) outperforms GDAS on CIFAR-100 and ImageNet-16-120 but underperforms slightly on CIFAR-10. The single-level results on this benchmark provides concrete support for our convergence analysis, which only applies to the ERM problem.

As noted in Section 5, the search space considered in this benchmark differs from the prior two in that there is no subsequent edge pruning. Additionally, the search space is fairly small with only 3 nodes for which architecture decisions must be made. The success of GAEA DARTS (ERM) on this benchmark indicate the need for a better understanding of when single-level optimization should be used in favor of the default bi-level optimization problem and how the search space impacts the decision.

B.4 Comparison to XNAS

As discussed in Section 1.1, XNAS is similar to GAEA in that it uses an exponentiated gradient update but is motivated from a regret minimization perspective. [37] provides regret bounds for XNAS relative to the observed sequence of validation losses, however, this is not equivalent to the regret relative to the best architecture in the search space, which would have generated a different sequence of validation losses.

XNAS also differs in its implementation in two ways: (1) a wipeout routine is used to zero out operations that cannot recover to exceed the current best operation within the remaining number of iterations and (2) architecture gradient clipping is applied per data point before aggregating to form the update. These differences are motivated from the regret analysis and meaningfully increase the complexity of the algorithm. Unfortunately, the authors do not provide the code for architecture search in their code release at <https://github.com/NivNayman/XNAS>. Nonetheless, we implemented XNAS [37] for the NAS-Bench-201 search space to provide a point of comparison to GAEA.

Our results shown in Figure 5 demonstrate that XNAS exhibits much of the same behavior as DARTS in that the operations all converge to skip connections. We hypothesize that this is due to the gradient clipping, which obscures the signal kept by GAEA in favor of convolutional operations.